



Science IN

Contents lists available at <http://www.jmsse.org/> & <http://www.jmsse.in/>

Journal of Materials Science and Surface Engineering



## Mechanical and Thermal Properties Evaluation of Nanocrystalline TiB<sub>2</sub> Added Epoxy-ZrO<sub>2</sub> Composites

V. Rangadhara Chary, M. K. Mohan

Department of MME, NIT Warangal, Telangana State, India.

### Article history

Received: 15-Mar-2017

Revised: 28-April-2017

Available online: 20-May-2017

### Keywords:

Epoxy composites,  
Glass Transition  
Temperature,  
Nanocrystalline TiB<sub>2</sub>,  
Self-propagating High-  
temperature Synthesis (SHS),  
Tensile and Flexural  
Properties,  
ZrO<sub>2</sub> powder

### Abstract

The present investigation aims at understanding the influence of nanocrystalline TiB<sub>2</sub> powder addition on mechanical properties of micron-sized ZrO<sub>2</sub> powders reinforced epoxy composites. The nanocrystalline TiB<sub>2</sub> powder is synthesized by self-propagating high temperature synthesis and is in the size range of 60-70 nm as revealed from TEM studies. The preparation of epoxy composites are done by hand-layout technique and are allowed to cure under vacuum at room temperature. The Epoxy-ZrO<sub>2</sub> microcomposites were casted using hand-layout technique and cured under vacuum at room temperature. The nanocomposites were prepared by addition of 0.2, 0.4, 0.6, 0.8, and 1.0 vol% TiB<sub>2</sub> to Epoxy-4 vol% ZrO<sub>2</sub> microcomposite. Ductility has increased by 3-4 times in comparison to neat epoxy, and it has increased by two times in comparison to microcomposites. The Vickers hardness of composites shows an increasing trend with increasing particulate content. DSC studies reveal the glass transition temperature, T<sub>g</sub>, of the epoxy composites to be lower than the neat epoxy and a decreasing trend was observed with increasing filler content.

© 2017 Science IN. All rights reserved

### Introduction

The research spectrum in the area of advanced epoxy composites was widely enhanced because of the various possibilities available to achieve tailor made properties by enormous combinations of reinforcements, curing agents, diluents and modifiers. Polymer processing technology can be used for shaping, molding or replication of the polymer-based composites enabling a low cost fabrication of components and devices. Similarly for over two decades, ceramic filled polymer composites have been the subject of extensive research. The inclusion of inorganic fillers into polymers for commercial applications is primarily aimed at the cost reduction and stiffness improvement [1].

A newly developed strategy offering promising results is to reinforce nano-sized particles into epoxy matrices such as carbon nanotubes and nanofibers, nanoclays, metal oxide nanoparticles, etc. [2-4] and make new materials with enhanced properties. The unique properties of the nanoparticles such as nanometric size, high specific surface areas (up to 1000 m<sup>2</sup>/g) and the possibility of combining them with conventional reinforcements have caused intense research in the field of nanocomposites. In the recent research investigations, it has been proved that the epoxy/nanocomposites demonstrate better mechanical and dielectric properties [5-6] when compared with neat epoxy and epoxy with micron-sized fillers at a lower loading concentration (1-10%). The Epoxy-ZrO<sub>2</sub> composites are widely used in electrical and electronic applications like for LED encapsulation to improve the light extraction efficiency [7].

The purpose of the present study is to understand the effect of micron sized ZrO<sub>2</sub> powder reinforced into epoxy matrix on thermal and mechanical properties, and on Epoxy-ZrO<sub>2</sub> microcomposites with the addition of ceramic nanocrystalline

TiB<sub>2</sub> powder synthesized by self-propagating high temperature synthesis (SHS). TiB<sub>2</sub> has a unique combination of properties, such as a low density of 4.52 g/cc, high microhardness (34 GPa) as well as good thermal and electrical conductivity [8].

### Experimental

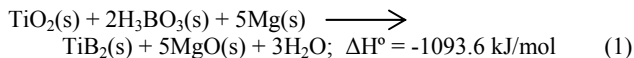
The epoxy resin used in the present work is Araldite LY556 with its corresponding anhydride hardener HY951, and both were supplied by Ciba Geigy India Ltd. The epoxy resin and the hardener are mixed in a ratio of 10:1 by weight. The density at 25°C of epoxy resin and hardener are 1.2 and 1.25 g/cc, respectively.

The ZrO<sub>2</sub> powder was obtained in 200 microns size from Loba Chemicals, India with a purity of 99.9%. TiO<sub>2</sub>, Boric acid, H<sub>3</sub>BO<sub>3</sub> (99.9% pure) and magnesium (99.9% pure, particle size <150µm) used for the synthesis of TiB<sub>2</sub> were also supplied by Loba Chemicals, India.

#### Synthesis of nanocrystalline TiB<sub>2</sub> powder by SHS process

The Self-propagating High-temperature Synthesis (SHS) technique to produce TiB<sub>2</sub> is highly attractive because of the relatively low temperature required to initiate the thermite reaction and faster reaction time in the order of nanoseconds. The stoichiometric thermite reaction between magnesium oxide (MgO), titanium dioxide (TiO<sub>2</sub>), and boric acid (H<sub>3</sub>BO<sub>3</sub>) produces a high purity titanium diboride (TiB<sub>2</sub>) and MgO as residual product. The chemical reaction occurs at a temperature of 680±15°C under Argon gas atmosphere in the tubular furnace chamber according to Equation 1. The as-reacted powders are made up of agglomerates with the MgO binding the hexagonal TiB<sub>2</sub> powder together.





The adiabatic temperature,  $T_{ad}$  for the above reaction is 3077°C [9]. After cooling, the synthesized powder was taken out. It was observed that the reacted mixture is in the form of black lumps, and some amount of white layer is formed on the lumps. The powder is crushed into fine powder before the leaching process. The leaching process [10] was carried out in dilute HCl with normality of 2N. The solution was mixed with the crushed powder and heated up to 120°C. In aqueous HCl, MgO reacts to form magnesium chloride and remains dissolved in the solution. The process was continued till the solution boils for about 10 min, and then the solution was separated from TiB<sub>2</sub> powder by using the filter paper. The resulting powder, which was taken after leaching process, was then dried in an oven for 1 h at 100°C.

#### Fabrication Methodology of Epoxy Composites

The fabrication of epoxy composites was carried out by casting using 'hand-layout technique'. For the casting process, molds are prepared using softwood board and plastic frame beads in the dimensions of 140x80x6mm (lxbxh). Before the beads are nailed on to the board, a transparent sheet is placed to ensure easy removal of the casting after solidification. The low temperature curing epoxy resin, Araldite LY556 and its corresponding hardener, HY951, are mixed in a ratio of 10:1 by weight as recommended. The 200µm ZrO<sub>2</sub> powder is weighed in different proportions of 2, 4, 6, 8, 10 vol% (Volume of the prepared mold) and are mixed in epoxy-hardener liquid compound by continuously stirring to ensure uniform mixing. Once the curing begins between the epoxy resin and hardener, which can be known with a slight increase in temperature, the liquid mixture is poured immediately into the prepared molds by ensuring for uniform thickness. The mold is then placed in a glove box in vacuum for 2 h to ensure the removal of any air bubbles entrapped during mixing. The castings were then stripped out of the mold and specimens of suitable dimensions were cut using a diamond cutter for further characterization. The fabrication of nanocomposites follows the same procedure, but care has been taken to mix ZrO<sub>2</sub> and TiB<sub>2</sub> powders homogeneously by manually milling them together using mortar mixer for 15 min before they are reinforced into epoxy resin. The compositions of micro and nanocomposites fabricated are given in Table 1.

**Table 1:** Compositions of Epoxy composites fabricated by hand-layout technique

Microcomposites		Nanocomposites
Epoxy-ZrO <sub>2</sub> Composites	Epoxy-TiB <sub>2</sub> Composites	Epoxy-ZrO <sub>2</sub> -TiB <sub>2</sub> Composites
Epoxy – 2 vol% ZrO <sub>2</sub>	Epoxy – 0.2 vol% TiB <sub>2</sub>	Epoxy – 4vol% ZrO <sub>2</sub> - 0.2 vol% TiB <sub>2</sub>
Epoxy – 4 vol% ZrO <sub>2</sub>	Epoxy – 0.4 vol% TiB <sub>2</sub>	Epoxy – 4 vol% ZrO <sub>2</sub> - 0.4 vol% TiB <sub>2</sub>
Epoxy – 6 vol% ZrO <sub>2</sub>	Epoxy – 0.6 vol% TiB <sub>2</sub>	Epoxy – 4 vol% ZrO <sub>2</sub> - 0.6 vol% TiB <sub>2</sub>
Epoxy – 8 vol% ZrO <sub>2</sub>	Epoxy – 0.8 vol% TiB <sub>2</sub>	Epoxy – 4 vol% ZrO <sub>2</sub> - 0.8 vol% TiB <sub>2</sub>
Epoxy – 10 vol% ZrO <sub>2</sub>	Epoxy – 1.0 vol% TiB <sub>2</sub>	Epoxy – 4 vol% ZrO <sub>2</sub> - 1.0 vol% TiB <sub>2</sub>

#### Property Evaluation Techniques

Theoretical density of the epoxy composites is calculated by using Rule-of-Mixtures. The experimental density of the epoxy composites were measured by Archimedes principle using a AXIS (Model: AGN300) digital balance with density measurement kit.

A sample of 20x10x5 mm is first weighed in air and then in double distilled water to know the Archimedes density. All the measurements were done at room temperature. The percentage error was 0.001% for the density measurements of the samples.

The Vickers hardness of the epoxy composites was measured using MATSUZAWA (Model: VMT-X) hardness testing machine. A load of 3 kg was applied with a dwell time for indentation of 30 sec. A total number of 10 indentations were taken on each sample and the average hardness value is reported.

The tensile and flexural properties were measured using TINIUS OLSEN universal testing machine (Model: H 10KS) with a load cell of 10 kN and at a constant strain rate of 2 mm/min. The dog-bone shape specimens for tensile testing were prepared according to ASTM D7205/D7205M-06 (2011) standards and flat specimens for flexural testing were prepared according to ASTM D790 standards. A total of five samples were tested for each composition and the average tensile strength and % elongation are recorded whereas a total of three specimens were tested using a span length of 70 mm for recording the average flexural strength and flexural modulus.

The glass transition temperature of epoxy composites was measured using a Differential Scanning Calorimeter (DSC) supplied by Pelkin Elmer (Model: DSC 8000). The weighed samples were placed in aluminum pans and secured with lids. The sample was then placed in DSC along with an empty reference pan. A constant flow of N<sub>2</sub> gas was allowed with a flow rate of 20 ml/min. The heating cycle started at 30°C with a heating rate of 10°C/min up to a temperature of 200°C. The normalized heat flow (W/g) curves were generated for determination of glass transition temperatures and these were measured by using half-C<sub>p</sub> method provided by Pyris Software.

Transmission Electron Microscopy (TEM) was used to know the particle size of synthesized TiB<sub>2</sub> powder using FEI make Tecnai G<sup>2</sup> TEM with EDS System. Samples for TEM studies were prepared initially by dispersing the powders in methanol using ultrasonic cleaner for 20-30 min. The particles were subsequently collected on the carbon coated copper grids and the foils were dried using UV lamp.

## Results and Discussion

#### Density Measurements

The theoretical and measured densities of micro and nanocomposites are shown in Tables 2-4. The void volume or % porosity of the composites was calculated according to ASTM D2734-09 standards using the following expression,

$$\% \text{ Porosity} = \frac{(\rho_t - \rho_m)}{\rho_m} \times 100$$

where,  $\rho_t$  and  $\rho_m$  are theoretical and measured composite density respectively.

The density of the neat epoxy was taken as 1.20 g/cc for all the calculations. The increase in the void volume with increasing filler content was due to the moisture absorption by the powders during mixing at room temperature. However the maximum porosity observed in the composites did not exceed 5% which is considered tolerable for property evaluation.

#### Mechanical Properties of Epoxy Composites

The Vickers hardness measurements were carried out to know the effect of addition of particulates on the hardness of the epoxy composites.

Table 5 shows the Vickers hardness values of the Epoxy-ZrO<sub>2</sub> microcomposites. The reported values are the average of 10 indentations taken on each sample. The results show an increasing

trend in hardness with increasing vol% of ZrO<sub>2</sub> particles upto 6vol% and then decreases. The maximum Vickers hardness observed was HV 24.1 in case of Epoxy-6vol% ZrO<sub>2</sub>microcomposite.

**Table 2:** Theoretical and measured densities of epoxy-ZrO<sub>2</sub> microcomposites

Composition	Theoretical Density (g/cc)	Measured Density (g/cc)	Porosity (%)
Epoxy-2% ZrO <sub>2</sub>	1.289	1.256	2.6
Epoxy-4% ZrO <sub>2</sub>	1.379	1.341	2.8
Epoxy-6% ZrO <sub>2</sub>	1.468	1.418	3.4
Epoxy-8% ZrO <sub>2</sub>	1.558	1.492	4.2
Epoxy-10% ZrO <sub>2</sub>	1.648	1.560	4.5

**Table 3:** Theoretical and measured densities of epoxy-TiB<sub>2</sub> nanocomposites

Composition	Theoretical Density (g/cc)	Measured Density (g/cc)	Porosity (%)
Epoxy-0.2% TiB <sub>2</sub>	1.206	1.201	0.4
Epoxy-0.4% TiB <sub>2</sub>	1.213	1.208	0.4
Epoxy-0.6% TiB <sub>2</sub>	1.219	1.210	0.6
Epoxy-0.8% TiB <sub>2</sub>	1.226	1.215	0.7
Epoxy-1.0% TiB <sub>2</sub>	1.233	1.217	1.3

**Table 4:** Theoretical and measured densities of epoxy-ZrO<sub>2</sub>-TiB<sub>2</sub> nanocomposites

Composition	Theoretical Density (g/cc)	Measured Density (g/cc)	Porosity (%)
Epoxy-4% ZrO <sub>2</sub> -0.2% TiB <sub>2</sub>	1.385	1.350	3.5
Epoxy-4% ZrO <sub>2</sub> -0.4% TiB <sub>2</sub>	1.392	1.343	4.9
Epoxy-4% ZrO <sub>2</sub> -0.6% TiB <sub>2</sub>	1.399	1.350	4.8
Epoxy-4% ZrO <sub>2</sub> -0.8% TiB <sub>2</sub>	1.405	1.362	4.3
Epoxy-4% ZrO <sub>2</sub> -1.0% TiB <sub>2</sub>	1.412	1.359	5.2

**Table 5:** Mechanical properties of neat epoxy and epoxy-ZrO<sub>2</sub> microcomposites

Composition	Vickers Hardness, HV	Tensile Strength, MPa	% Elongation	Flexural Strength, MPa	Flexural Modulus, GPa
Neat Epoxy	18.7	62.4	1.06	80.70	2.37
Epoxy-2% ZrO <sub>2</sub>	21.6	21.69	2.01	78.06	4.94
Epoxy-4% ZrO <sub>2</sub>	23.5	32.50	2.30	93.41	5.58
Epoxy-6% ZrO <sub>2</sub>	24.1	30.72	1.99	88.22	4.88
Epoxy-8% ZrO <sub>2</sub>	23.4	22.63	1.89	77.11	4.75
Epoxy-10% ZrO <sub>2</sub>	23.1	21.58	1.65	57.16	3.66

Fig.1 shows the variation of Vickers Hardness of Epoxy-TiB<sub>2</sub> (Table 6) and Epoxy-4%ZrO<sub>2</sub>-TiB<sub>2</sub> (Table 7) nanocomposites with

increasing vol% of nanocrystalline TiB<sub>2</sub>. It is clear from the results that with the addition of nano TiB<sub>2</sub>, the hardness was increased with increasing filler content in both the cases. The Epoxy-4vol%ZrO<sub>2</sub>-1.0vol%TiB<sub>2</sub> nanocomposite shows a hardness value of HV26.6, even with a considerable amount of porosity involved i.e., 5.2%. In a study by Man-Wai Hoet al, [11] the Vickers hardness of 5 wt% nanoclay filled epoxy composites is very low, i.e., HV 11.3, when compared to the hardness achieved by addition of only 1.0 vol% ZrO<sub>2</sub> in Epoxy-4 vol% ZrO<sub>2</sub>-1.0 vol% TiB<sub>2</sub> nanocomposites. The results show an encouraging trend in improving the hardness with the addition of small volume fractions of nano TiB<sub>2</sub> to brittle epoxy matrix.

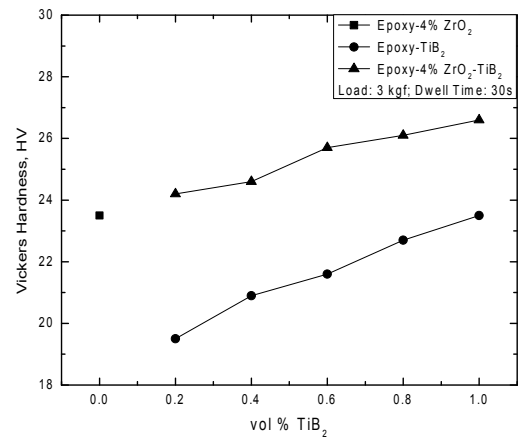


**Figure 1:** Variation of hardness of Epoxy nanocomposites with the addition of nano TiB<sub>2</sub>

**Table 6:** Mechanical Properties of Epoxy-TiB<sub>2</sub> nanocomposites

Epoxy-TiB <sub>2</sub>	Vickers Hardness, HV	Tensile Strength, MPa	% Elongation	Flexural Strength, MPa	Flexural Modulus, GPa
Epoxy-0.2%TiB <sub>2</sub>	19.5	47.05	1.35	64.17	3.78
Epoxy-0.4%TiB <sub>2</sub>	20.9	40.11	2.19	62.86	3.74
Epoxy-0.6%TiB <sub>2</sub>	21.6	38.36	2.32	58.17	3.66
Epoxy-0.8%TiB <sub>2</sub>	22.7	37.89	2.41	43.54	3.11
Epoxy-1.0%TiB <sub>2</sub>	23.5	32.92	2.48	36.39	2.95

**Table 7:** Mechanical Properties of Epoxy-ZrO<sub>2</sub>-TiB<sub>2</sub> Nanocomposites

Composition	Vickers Hardness, HV	Tensile Strength, MPa	% Elongation	Flexural Strength, MPa	Flexural Modulus, GPa
Epoxy-4%ZrO <sub>2</sub> -0.2%TiB <sub>2</sub>	24.2	30.1	3.72	94.04	5.61
Epoxy-4%ZrO <sub>2</sub> -0.4%TiB <sub>2</sub>	24.6	30.8	3.81	94.37	5.63
Epoxy-4%ZrO <sub>2</sub> -0.6%TiB <sub>2</sub>	25.7	27.2	4.01	94.81	5.68
Epoxy-4%ZrO <sub>2</sub> -0.8%TiB <sub>2</sub>	26.1	25.3	4.11	95.16	5.70
Epoxy-4%ZrO <sub>2</sub> -1.0%TiB <sub>2</sub>	26.6	24.6	4.13	95.23	5.71

Table 5 shows the effect of ZrO<sub>2</sub> content on the tensile strength and ductility of Epoxy-ZrO<sub>2</sub>microcomposites. It can be seen, from Fig. 2 that the tensile strength has increased and then decreased while there is a considerable increase of about two times in ductility with increasing volume fraction of ZrO<sub>2</sub> particles in

comparison with neat epoxy. The optimum values for tensile strength and ductility were achieved at 4 vol% loading of ZrO<sub>2</sub> particles i.e., 32.50 MPa and 2.30% respectively. The decrease in tensile strength with increasing ductility indicates the change in brittle to ductile nature of these microcomposites. The huge increase in ductility when compared to neat epoxy is attributed to the crack branching that occurs because of the ductile particles embedded inside a brittle epoxy matrix. It is well documented that good interfacial adhesion can provide better stress transfers to the ZrO<sub>2</sub> particles in the composites, and this will improve the strength and ductility of the composites [12-13].

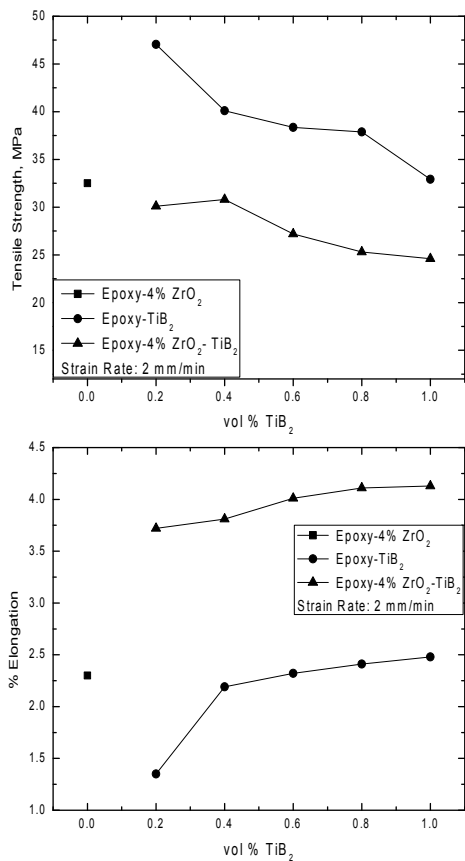


**Figure 2:** Effect of nano TiB<sub>2</sub> addition on tensile properties of Epoxy nanocomposites, a) Tensile strength b) Elongation

The tensile strength and ductility of microcomposites has greatly influenced by the addition of nanocrystalline TiB<sub>2</sub>. It is evident from the Fig2 that the tensile strength has decreased with increasing the volume fraction of the nano TiB<sub>2</sub> in both Epoxy-TiB<sub>2</sub> (Table 6) and Epoxy-ZrO<sub>2</sub>-TiB<sub>2</sub> (Table 7) composites which is attributed to the crack branching phenomenon. It is well known that nanoparticles influence the crack branching more effectively than micron sized particles. In a study by Saidina *et al* [14] with calcium copper titanate and barium titanate reinforced epoxy composites, the reported tensile strength is about 40 MPa and 55 MPa respectively at 5 vol% loading, which is very low compared to the tensile strength of 40-47 MPa achieved in the case of Epoxy-TiB<sub>2</sub> nanocomposites with only 0.2-0.4 vol% addition of TiB<sub>2</sub>. In another study by Luyt *et al* [15] using copper powder filled low-density (LDPE) and linear low-density (LLDPE) polyethylene composites, the tensile strength was reported as 8.3 MPa and 17.9 MPa with 4 vol% Cu loading in LDPE and LLDPE respectively. The tensile strength achieved in the present study using 4 vol% ZrO<sub>2</sub> i.e., 31.63 MPa, in epoxy matrix is comparably

high to Luyt *et al* which explain the good adhesion of ZrO<sub>2</sub> particles in epoxy matrix than in LDPE or LLDPE polymer matrix. The ductility of the nanocomposites has considerably increased by about 2 times in case of Epoxy-TiB<sub>2</sub> nanocomposites and by about 3-4 times in case of Epoxy-ZrO<sub>2</sub>-TiB<sub>2</sub> nanocomposites. The increase in ductility indicates the uniform distribution of nanoparticles in these nanocomposites.

The flexural properties of the specimens were carried out by Three-Point Bend Test with a span length of 70 mm. The flexural strength of Epoxy-ZrO<sub>2</sub> microcomposites increased and then decreased with increasing ZrO<sub>2</sub> content, and the flexural modulus shows an increasing trend up to 4 vol% ZrO<sub>2</sub> and then decreases as evident from Table 5. In the presence of ZrO<sub>2</sub> particles, the stress fields change locally and thus may suppress cavitation deformation modes at least to some extent and instead may initiate local shear yielding of the surrounding matrix as discussed by Dekkers *et al* [16].

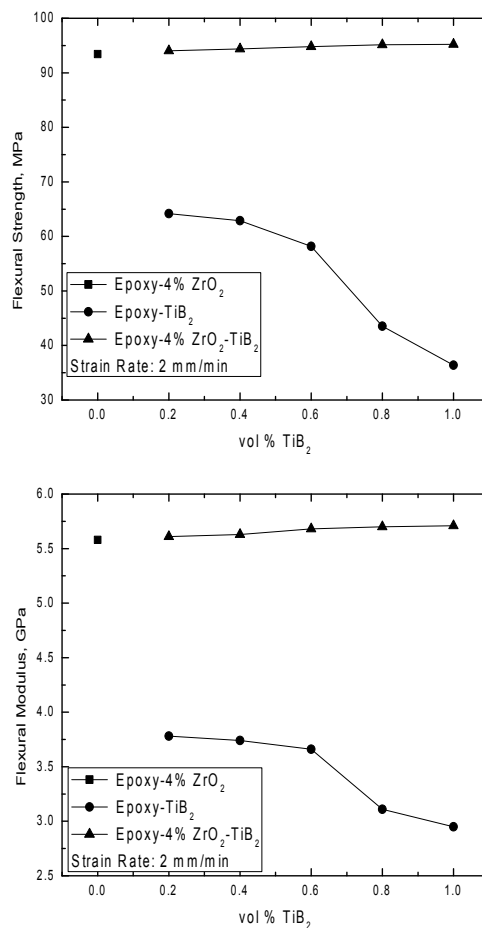


**Figure 3:** Flexural properties of Epoxy nanocomposites with the addition of nano TiB<sub>2</sub> a) Flexural Strength, b) Flexural Modulus

The flexural strength and flexural modulus of Epoxy-TiB<sub>2</sub> nanocomposites is given in Table 6 and Fig 3. From the data, it is clear that both the flexural properties have decreased with increasing TiB<sub>2</sub> volume fraction. This is because the nanocrystalline TiB<sub>2</sub> usually assists the stress transfer between particles and matrix by crack branching phenomenon.

The flexural properties of Epoxy-ZrO<sub>2</sub>-TiB<sub>2</sub> nanocomposites, Table 7 and Fig 3, show an increasing trend in both flexural strength and flexural modulus with increasing volume fraction of nano TiB<sub>2</sub>. The high flexural modulus indicates the strong bonding



between the ZrO<sub>2</sub> particles and the epoxy matrix. The reported flexural modulus of recycled Cu reinforced epoxy composites i.e., 2.5-3.0 GPa at 10 vol% and 3.5-4.0 GPa at 40 vol% loading [17], is very low when compared with the achieved flexural modulus of 5.61-5.71 GPa with the addition of relatively small amounts of nano TiB<sub>2</sub> i.e., 0.2-1.0 vol% TiB<sub>2</sub> to Epoxy-4 vol% ZrO<sub>2</sub> microcomposites. The propagation of the crack is impeded by the stiff particles that act as obstacles slowing down the advancing of the crack front by localized shear yielding.

The mechanical behavior of epoxy composites greatly depend on the stresses and strains encountered during tensile and flexural tests along with dewetting. Dewetting is the phenomenon where new voids are created because of poor interfacial adhesion or because of breaking up of aggregates in particulate reinforced epoxy composites [18].

#### Differential Scanning Calorimetry (DSC) Studies

Thermoset resins exhibit glass transition, which is thermodynamically a second order transition, at which a second derivative of free energy (volume, heat capacity) vs. temperature plot is continuous. The second derivative of free energy (volume, heat capacity) vs. temperature plot is discontinuous for melting. Glass transition results from segmental motion called  $\alpha$ -relaxation. As the temperature increases the free volume increases and, at a certain temperature, the free volume becomes sufficient to initiate segmental motion. This temperature is called the glass transition temperature ( $T_g$ ). Some relaxation, called  $\beta$ -relaxation, takes place below  $T_g$ .

DSC spectra give information about any thermal change during the heating regime. In the glass transition region, the heat capacity drastically changes, which is manifested as a shift in base line of the DSC spectra. The mid-point of the shift curve is taken as  $T_g$ . In the case of a thermoset, the molecular weight of the network is infinity. However,  $T_g$  depends on various factors, such as the nature of the curing agent, curing time, and curing conditions. For example, DiGlycidyl Ether of Bisphenol A (DGEBA) epoxy resin exhibits  $T_g$  in the range of -30 to 200 °C depending on the nature of curing agents [19].

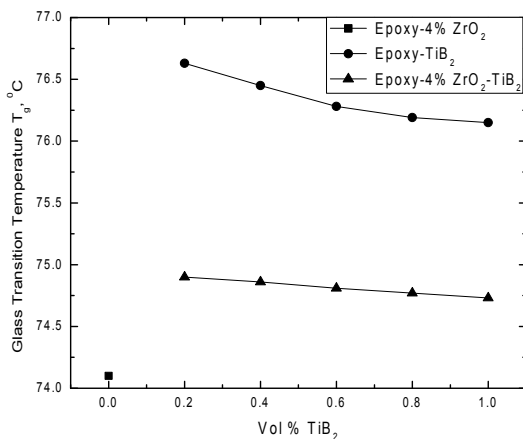


**Figure 4:** Variation in  $T_g$  of nanocomposites with the addition of nano TiB<sub>2</sub>

The measured glass transition temperatures of microcomposites and nanocomposites are presented in the Tables 8 and 9 respectively. Fig 4 shows the change in glass transition temperature with varying TiB<sub>2</sub> content. In case of Epoxy-ZrO<sub>2</sub> microcomposites, the addition of ZrO<sub>2</sub> powder into epoxy matrix shows an increasing trend of  $T_g$  from 74.02°C to 74.78°C with increasing volume fraction of ZrO<sub>2</sub>. This is because of ZrO<sub>2</sub>

particles acting as heat sinks resulting in higher  $T_g$  as revealed from the increased heat flow. Further, with increasing filler content the  $T_g$  has slightly decreased in both Epoxy-TiB<sub>2</sub> and Epoxy-ZrO<sub>2</sub>-TiB<sub>2</sub> nanocomposites as shown in Table 9. The reduction in the  $T_g$  suggests that the presence of ZrO<sub>2</sub> and TiB<sub>2</sub> particles within the structure provides confinement of polymer chains mobility which acts as barrier that prevents some cross-linking from occurring i.e., decreased free volume for cross-linking. The subsequent reduction in cross-linking and decreased free volume has shown the effect of lowering the  $T_g$ . In comparison to Al<sub>2</sub>O<sub>3</sub> particles, nanocrystalline TiB<sub>2</sub> particles are most effective in decreasing the cross-linking probability of epoxy and since TiB<sub>2</sub> in nano size invariably decreased the free volume of epoxy showing its good dispersion tendency than Al<sub>2</sub>O<sub>3</sub> particles [20].

#### Transmission Electron Microscopy (TEM) Studies

TEM images of nanocrystalline TiB<sub>2</sub> powder reveal the particle size to be in the range of 60-70 nm. The hexagonal crystal structure of the TiB<sub>2</sub> powder can be observed in Selected Area Diffraction (SAD) pattern and the hexagonal morphology can also be seen in the TEM images, Fig 5. Extensive TEM study of synthesized SHS TiB<sub>2</sub> powder by Saikumar G [21] confirms the obtained nano particle size range in the present study.

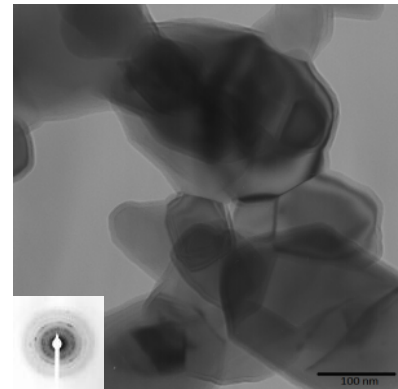


**Figure 5:** TEM micrographs and SAD pattern of nanocrystalline TiB<sub>2</sub> powder (Mag 150 kX)

**Table 8:** Glass Transition Temperature,  $T_g$  of Neat Epoxy and Epoxy-ZrO<sub>2</sub> microcomposites

Composition	$T_g$ , °C
Neat Epoxy	77.44
Epoxy-2%ZrO <sub>2</sub>	74.02
Epoxy-4%ZrO <sub>2</sub>	74.10
Epoxy-6%ZrO <sub>2</sub>	74.12
Epoxy-8%ZrO <sub>2</sub>	74.59
Epoxy-10%ZrO <sub>2</sub>	74.78

**Table 9:** Glass Transition Temperature,  $T_g$  of Epoxy Nanocomposites

Epoxy-TiB <sub>2</sub>	$T_g$ , °C	Epoxy-ZrO <sub>2</sub> -TiB <sub>2</sub>	$T_g$ , °C
Epoxy-0.2%TiB <sub>2</sub>	76.63	Epoxy-4%ZrO <sub>2</sub> -0.2%TiB <sub>2</sub>	74.90
Epoxy-0.4%TiB <sub>2</sub>	76.45	Epoxy-4%ZrO <sub>2</sub> -0.4%TiB <sub>2</sub>	74.86
Epoxy-0.6%TiB <sub>2</sub>	76.28	Epoxy-4%ZrO <sub>2</sub> -0.6%TiB <sub>2</sub>	74.81
Epoxy-0.8%TiB <sub>2</sub>	76.19	Epoxy-4%ZrO <sub>2</sub> -0.8%TiB <sub>2</sub>	74.77
Epoxy-1.0%TiB <sub>2</sub>	76.15	Epoxy-4%ZrO <sub>2</sub> -1.0%TiB <sub>2</sub>	74.73

#### Conclusion

It can be concluded from the present study that the reinforcement of nanocrystalline TiB<sub>2</sub> powder into Epoxy-ZrO<sub>2</sub> microcomposites will improve the thermal and mechanical properties appreciably. The addition of nanocrystalline TiB<sub>2</sub> powder has improved the ductility of the Epoxy-ZrO<sub>2</sub> microcomposites by about 3-4 times without much affecting the strength properties. The Vickers hardness was also found to increase with the addition of TiB<sub>2</sub> particles to the microcomposites. The TEM micrographs along with the SAD pattern reveal the nano particle size and hexagonal crystal structure of the synthesized TiB<sub>2</sub> particles. DSC studies show the decrease in glass transition temperature in both micro and nanocomposites with increasing filler content i.e., nanocrystalline TiB<sub>2</sub>.

## References

1. Rothon R N, Mineral fillers in thermoplastics: filler manufacture, *J. Adhesion*, 64 (1997) 87-109.
2. Fothregill J C, Nelson J K, Fu M, "Dielectric properties of epoxy nanocomposites containing TiO<sub>2</sub>, Al<sub>2</sub>O<sub>3</sub> and ZnO fillers", Annual Report Conference on Electrical insulation and dielectric phenomena (CEIDP), Boulder, CO, October (2004).
3. Lewis T J, "Interfaces and nanodielectrics are synonymous", Proceedings of the 2004 IEEE international conference on solid dielectrics, Toulouse, July (2004).
4. Nelson J K, Hu Y, "The impact of nanocomposite formulations on electrical voltage endurance", Proceedings of the 2004 IEEE international conference on solid dielectrics, Toulouse, July (2004).
5. Singha S, Thomas M J, "Dielectric properties of epoxy nanocomposites", *IEEE T. Dielect. El. In.*, 15 (2008), 12-23.
6. Tanaka T, "Dielectric nanocomposites with insulating properties", *IEEE T. Dielect. El. In.*, 12-5 (2005), 914-928.
7. P T Chung, C T Yang, S H Wang, C W Chen, Anthony S T Chiang, Cheng-Yi Liu, "ZrO<sub>2</sub>/epoxy nanocomposite for LED encapsulation", *Materials Chemistry and Physics*, 136 (2012), 868-876.
8. Chen H, Zhang J, Fu Z, Influence of Fe/Ni/Al additive on the sintering behaviors of TiB<sub>2</sub>cermets, *J. Wuhan Univ. Technol. Mater. Sci. Ed.*, 24 (2009) 879-882.
9. Sundaram V, Logan K V, Speyer R F, Reaction path in the magnesium thermite reaction to synthesize titanium diboride, *J. Mat. Research*, 12-10 (1997) 2657-2664.
10. SaikumarGadakary, Asit K Khanra, Veerababu R, Production of nanocrystalline TiB<sub>2</sub> powder through self-propagating high temperature synthesis (SHS) of TiO<sub>2</sub>-H<sub>3</sub>BO<sub>3</sub>-Mg mixture, *Adv. Appl. Ceram.*, 113 (2014) 419-426.
11. Man-Wan Ho, Chun-Ki Lam, Kin-tak Lau, Dickon H L Ng, David Hui, "Mechanical Properties of epoxy-based composites using nanoclays", *Composite Structures*, 75 (2006), 415-421.
12. Lin L-Y, Lee J-H, Hong C-E, Yoo G-H, Advani S G, Preparation and characterization of layered silicate/glass fiber/ epoxy hybrid nanocomposites via vacuum-assisted resin transfer molding (VARTM), *Compos. Sci. Tech.*, 66 (2006) 2116-2125.
13. Karippal J J, Narasimha Murthy H N, Rai K S, Sreejith M, Krishna M, Study of mechanical properties of epoxy/glass/nanoclay hybrid composites, *J. Compos. Matls*, 45-18 (2011) 1893-1899.
14. Saidina D S, Mariatti M, Julie M J, Properties of calcium copper titanate and barium titanate filled epoxy composites for electronic applications: effect of filler loading and hybrid fillers, *J Mater Sci: Mater Electron*, 25 (2014) 4923-4932.
15. Luyt A S, Molefi J A, Krump H, Thermal, Mechanical and electrical properties of copper powder filled low-density and linear low-density polyethylene composites, *Polymer Degradation and Stability*, 91 (2006) 1629-1636.
16. Dekkers, M E J, Heikens D, Crazing and Shear deformation in glass bead-filled glassy polymers, *Journal of Materials science*, 20 (1985) 3873-3880.
17. Pargi M N F, Teh P L, Hussiensyah S, Yeoh C K, Ghani S A, Recycled-copper-filled epoxy composites: the effect of mixed particle size, *Intl J of Mech and Materials Engg*, 10-3 (2015).
18. Tavman I H, Thermal and mechanical properties of copper powder filled poly (ethylene) composites, *J. Powder Tech.*, 91 (1997) 63-67.
19. Qipeng Guo (Ed), *Thermosets: Structure, properties and application*, Woodhead Pub. Ltd (2012).
20. Alok Agrawal, AlokSatapathy, Experimental investigation of micro-sized aluminium oxide reinforced epoxy composites for microelectronic applications, *Procedia MatlsSci*, 5 (2014) 517-526.
21. Saikumar Gadakary, Synthesis of Borides powder and deformation behavior of boride based composites, PhD Thesis, NIT Warangal, India (2015).

